

SCALE EFFECT OF CONTAMINANT TRANSPORT IN SATURATED POROUS MEDIA IDENTIFIED BY
THE TIME FRACTIONAL ADVECTION-DISPERSION EQUATION

by

RHIANNON GARRARD

YONG ZHANG, COMMITTEE CHAIR

GEOFFREY TICK

YUEHAN LU

EBEN BROADBENT

A THESIS

Submitted in partial fulfillment of the requirements
for the degree of Master of Science
in the Department of Geological Sciences
in the Graduate School of
The University of Alabama

TUSCALOOSA, ALABAMA

2017

Copyright Rhiannon Garrard 2017
ALL RIGHTS RESERVED

ABSTRACT

Time nonlocal transport models such as the time fractional advection-dispersion equation (t-fADE) were proposed to capture well-documented non-Fickian dynamics for conservative solutes transport in heterogeneous media, with the underlying assumption that the time nonlocality (which means that the current concentration change is affected by previous concentration load) embedded in the physical models can release the effective dispersion coefficient from scale dependency. This assumption however has never been systematically examined using real data. This study fills this historical knowledge gap by capturing non-Fickian transport (likely due to solute retention) documented in literature (Huang et al. 1995) and observed in our laboratory from small to intermediate spatial scale using the promising, tempered t-fADE model. Fitting exercises show that the effective dispersion coefficient in the t-fADE, although differing subtly from the dispersion coefficient in the standard advection-dispersion equation, increases nonlinearly with the travel distance (varying from 0.5 to 12 m) for both heterogeneous and macroscopically homogeneous sand columns. Further analysis reveals that, while solute retention in relatively immobile zones can be efficiently captured by the time nonlocal parameters in the t-fADE, the retention-independent solute movement in the mobile zone is affected by the spatial evolution of local velocities in the host medium, resulting in a scale-dependent dispersion coefficient. The same result may be found for the other standard time nonlocal transport models, such as the well-known multi-rate mass transfer (MRMT) model and the hydrologic version of

continuous time random walk (CTRW), that separate solute retention and jumps (i.e., displacement).

Therefore, the t-fADE with a constant dispersion coefficient cannot capture scale-dependent dispersion in saturated porous media, challenging the application for stochastic hydrogeology methods in quantifying real-world, pre-asymptotic transport. Hence, improvements on time nonlocal models using, for example the novel subordination approach, are necessary to incorporate the spatial evolution of local velocities without adding cumbersome parameters. Future improvements are also explored, given knowledge obtained in this study.

LIST OF ABBREVIATIONS AND SYMBOLS

c	concentration
t	time
x	distance
v	velocity
D	hydrodynamic dispersion
α	dispersivity
β	capacity coefficient
γ	time index
λ	time truncation parameter
M_0	initial tracer mass
A	cross sectional area
θ	porosity

ACKNOWLEDGEMENTS

Thank you to everyone who supported this thesis including my advisor Dr. Yong Zhang and the rest of my committee and others who contributed including Jiazhong Qian, HongGuang Sun and Song Wei. Another thanks to Bingqing Lu for keeping me company in the lab as we did our research together, and of course my family who are always behind the scenes.

CONTENTS

ABSTRACT	ii
LIST OF ABBREVIATIONS AND SYMBOLS	iv
ACKNOWLEDGEMENTS.....	v
LIST OF TABLES	viii
LIST OF FIGURES.....	ix
1 INTRODUCTION	1
1.1 Background.....	1
1.2 Previous Work	2
1.3 Specific Questions and Aims	5
1.4 Outline of Chapters.....	5
2 METHODOLOGY.....	7
3 APPLICATION.....	9
3.1 Small Scale Laboratory Experiment.....	9
3.2 Intermediate Scale Literature Data	11
3.3 Issues comparing the t-fADE and ADE	13
4 RESULTS.....	15
4.1 Small scale.....	15
4.2 Intermediate Scale	18
5 DISCUSSION.....	24

5.1	The t-fADE Model Cannot Capture Scale-Dependent Dispersion	24
5.2	Comparison to Other Models and Possible Solutions for Scale-Dependent Dispersion	28
5.3	Discrepancy between Small- and Intermediate-Scale Laboratory Experiments.....	29
5.4	Dispersivity as a Linear Regression.....	30
5.5	Need of a Paradigm shift in numerical modeling of non-Fickian transport?.....	33
6	CONCLUSION.....	36
	REFERENCES.....	37
	APPENDIX: Finite Difference Solution for the T-fADE model.....	43

LIST OF TABLES

1. Velocity, dispersion, and dispersivity values from the 1-m glass beads column18

2. Velocity, dispersion, and dispersivity values from the 1-m quartz grain column18

3. Velocity, dispersion, and dispersivity values from the 12-m homogeneous sand column20

4. Velocity, dispersion, and dispersivity values from the 12-m heterogeneous sand column23

5. Values for β , γ and λ (in the t-fADE model) held constant for each 12-m column23

LIST OF FIGURES

1. Set-up of the 1-meter columns.....	10
2. Intermediate Scale, heterogeneous column set-up	12
3. Fittings for the 1-m glass bead column.....	17
4. Fittings for the 1-m quartz grain column.....	19
5. Fit of the t-fADE (solid lines) on the 12-m homogeneous column at half meter intervals.....	21
6. Fit of the t-fADE on the 12-m heterogeneous column at meter intervals.....	24
7. Best-fit velocity at the 12-m intermediate scale.....	26
8. Best-fit log dispersion at the 12-m intermediate scale	26
9. Best-fit log dispersivity at the 12-m intermediate scale.....	27
10. A log-log plot of dispersivity with distance from all four column experiments	32

1. INTRODUCTION

1.1 Background

Successfully monitoring groundwater quality and its subsequent remediation requires the development of reliable models, capable of predicting the spread of contaminant plumes. The key issue, hindering the development of such models is the ubiquitously heterogeneous nature of geologic media causing scale dependency in contaminant transport which cannot be captured by the standard advection-dispersion equation (ADE) with a constant dispersion coefficient.

The ADE defines physical transport in saturated porous media by two types of motion: advection and hydrodynamic dispersion. Advection accounts for solute displacement driven by the (local) mean velocity, while hydrodynamic dispersion captures local motion deviating from the mean plus molecular diffusion, and can be thought of as a random process. Diffusive flux is modelled as a Fickian process, based on Fick's second law of diffusion. The hydrodynamic dispersion coefficient (D) is a sum of molecular diffusion (D^*) and mechanical dispersion: $D = \alpha v + D^*$, where α is dispersivity, a variable used to quantify the magnitude of deviation from mean velocity (v) based on the degree of heterogeneity inherent in the medium (Neuman and Di Federico 2003). Yet, despite the dispersion coefficient being modeled as a constant in the assumed Fickian process, in practice it exhibits non-Fickian scale dependency (Pickens and Grisak 1981; LaBolle and Fogg 2001; Serrano 1995; Gelhar et al. 1992; Brouwers 2012). More specifically it has been shown to be time dependent (Zhou and Selim 2003).

In macroscopically homogeneous porous media with a low variance and a short

correlation for rock permeability, such as glacial loess, dispersivity may eventually reach its Fickian asymptote (Garabedian et al 1988; Hess et al. 1992) due to the central limit theory. However, in heterogeneous systems (which sometimes can even exhibit non-stationary heterogeneity due to the change of depositional environment or sediment supply), such as braided stream deposits, non-Fickian transport tends to be persistent with a divergent plume variance and hence a stable dispersivity may never be reached (Serrano 1995; LaBolle and Fogg 2001). It is assumed that the non-Fickian transport behavior is directly related to the increase in dispersive transport (Van Genuchten and Wierenga 1976), or more recently, multi-rate mass transfer between the mobile zone and multiple immobile zones (Haggerty et al. 2000; Zhang et al. 2015).

1.2 Previous Work

Efficient quantification of scale-dependent transport remains a historical challenge in the hydrological sciences beginning in the 1980s when the scale issue was first identified (Pickens and Grisak 1981; Kopelman 1988; Dagan 1989; Neuman 1990; Van Wesenbeeck and Kachanoski 1991; Gelhar 1993; Zhang 2002; Haggerty et al. 2004; Hadley and Newell 2014; among many others). The challenge of quantifying soil heterogeneity has favored the advancement of stochastic models, which rely on random probability rather than discrete parameterization. Early stochastic models attempted to relate dispersivity, α , as a representation of microscopic variation with hydraulic conductivity (K) a macroscopic representation of variation from Darcy's Law (Dagan 1982; Gelhar and Axness 1983; Gelhar et al., 1983; Cushman 1987; Neuman 1990; Gelhar 1992; Hess 1992). Yet, large scale field experiments also conducted at this time demonstrated no significant correlation between α and K (Hess et al., 1988; Gelhar 1992). Findings from the MADE site, in particular, revealed that α remained

independent of K even with the use of high resolution grid space measurement, due to ever smaller preferential flow paths created by local heterogeneities (Zheng et al. 2011; Molz 2015). However, the transition between hydrofacies units with distinct K values did have a significant impact on dispersion which had, previously, not been well realized by conventional statistics or the ADE (LaBolle and Fogg 2001; Zinn and Harvey 2003).

Acknowledging the role of hydraulic conductivity transitions in the formation of distinct flow networks encouraged the development of “dual domain” models, initially conceptualized by Coats and Smith (1964) and Van Genuchten and Wierenga (1979). Dual domain models explain non-Fickian transport by assuming separation between stagnant diffusive zones and motile advective channels (Koch and Brady 1984; Cardenas 2009; Chaudhary et al. 2013), motivating the development of stochastic hydrogeology methods such as the time-nonlocal transport theories (Cushman 2002; Berkowitz et al. 2006; Zhang et al. 2009; Neuman and Tartovsky 2009). Representative time-nonlocal transport models include the multi-rate mass transfer (MRMT) model (Haggerty and Gorelick 1995; Haggerty et al. 2000), the continuous time random walk (CTRW) framework in hydrology (Berkowitz et al. 2006), and the time fractional advection-dispersion equation (t-fADE) model (Schumer et al. 2003; Meerschaert et al. 2008; Zhang et al. 2015).

Theoretically, time nonlocal models can release the dispersion coefficient’s dependence on travel distance, since they utilize upscaling methods. Time nonlocal transport models typically separate solute transport into one mobile advective zone and multiple parallel stagnant zones where solute particles are trapped for random periods (Metzler and Klafter 2000). For example, the t-fADE is built on CTRW framework, which assumes that heterogeneities exist at all scales and divides transport into various waiting times between successive solute particle

jumps (Benson et al. 2000; Berkowitz et al. 2006). Solute transport is then quantified by deriving empirical, spatially averaged, probability density functions for waiting times (Berkowitz et al. 2006). Therefore, it is possible that the major parameters in the t-fADE model, as well as the CTRW framework, do not vary with local medium properties.

The fADE models can be considered subsets of the CTRW framework. Details of these models can be found in Metzler and Klafter (2000), and Berkowitz (2002). Their primary improvement over the ADE is the use of fractional memory functions which allow for levy flight in place of Brownian motion. Thereby they allow both subdiffusion and superdiffusion. While the CTRW and other fADE models have been tested with laboratory experiments, the t-fADE is specifically tailored to model subdiffusion due to solute retention, the most common mode of transport in saturated heterogeneous porous media (Meerschaert et al. 2008; Zhang et al. 2009).

Unlike the other CTRW based models it is specifically time nonlocal as opposed to space nonlocal. Previous research on the model, including quantitative analysis and field simulation, has shown it to be capable of capturing heavy tailed breakthrough curves (BTCs) for passive tracers (Meerschaert et al. 2008; Zhang et al. 2009). However, no systematic validation has been conducted for the time nonlocal transport models using, for example, well-controlled laboratory experiments. This historical knowledge gap motivates this study.

In addition, although stochastic hydrogeology methods have been proposed for decades, their practical applications remain rather rare compared to the “problematic” ADE models with embedded grid-scale heterogeneity used routinely in hydrologic modeling (Zheng et al. 2011; Molz 2015). Possible reasons for the limited application of the stochastic hydrogeology methods were investigated recently, including, for example, the lack of education in stochastic hydrology and the lack of efficient models available for reactive transport in real aquifers

(Sanchez-Vila and Fernàndez-Garcia 2016). However, the fundamental assumptions of stochastic hydrogeological methods have not been scrutinized systematically: can time nonlocal transport models, such as the t-fADE with constant parameters, capture real-world scale-dependent dispersion for nonreactive tracers?

1.3 Specific Questions and Aims

The primary question of this thesis research is how the t-fADE as a time nonlocal model, which accounts for solute retention effects, interprets the scale dependency of the dispersion coefficient. A secondary question is how the results may apply more generally to other time nonlocal models. A positive result, improving scale dependency, would open doors for further development of time nonlocal models and expansion of stochastic methods in the field of computational hydrology. Otherwise, no improvement would indicate the need for a reflection on the issue of pre-asymptotic dispersion and the ADE, the direction of future research in the field of hydrology, and the place of stochastic models going forward.

In particular, this work aims to explore the scale-evolution of the effective dispersion coefficient in the t-fADE model using solute transport data obtained directly from well-controlled laboratory sand column experiments. Here, the t-fADE will be tested by modeling non-Fickian transport data observed in the laboratory from small (0.5 m) to intermediate (12 m) scales. The 12-m length scale is considered intermediate since most laboratory sand columns are less than 10 m.

1.4 Outline of Chapters

The remainder of this thesis is organized as follows. First, a full explanation of the t-fADE is given in the methodology section. Following is a description of the sand column experiments and

their properties in the application section. Results and discussion are given in their respective sections for outcome of the effects of the t-fADE on velocity and the dispersion. A finite-difference based Eulerian solver of the t-fADE model is shown in Appendix for interested readers.

2. METHODOLOGY

The t-fADE model (with a potential upper limit for solute residence times) was developed to account for solute retention due to mobile/immobile mass exchange (Meerschaert et al. 2008). It divides particle transport into discrete jump distances and waiting time periods. The t-fADE utilizes a temporal fractional-order derivative to characterize complex waiting time distributions which leads to a broad distribution of possible jump distances for solute particles (Metzler and Klafter 2000). This allows solute particles to exhibit larger variations from mean waiting times, obeying Lévy motion in the time domain (Pachepsky et al. 2000). The t-fADE, therefore, differs from the standard spatial fADE model in that it can account for subdiffusion due to the ubiquitous retention processes.

Equation 1 details the t-fADE model:

$$\frac{\partial c}{\partial t} + \beta e^{-\lambda t} \frac{\partial^\gamma}{\partial t^\gamma} (e^{\lambda t} c) = -v \frac{\partial c}{\partial x} + D \frac{\partial^2 c}{\partial x^2} \quad (1)$$

where c [ML^{-3}] is concentration, t [T] is time, D [LT^{-1}] is the dispersion coefficient, v [LT^{-1}] is seepage velocity, and x [L] is distance. Parameters not found in the standard ADE include β [$T^{\gamma-1}$], the fractional capacity coefficient which reflects the skew of the chemical plume (i.e. the spatial distribution of chemicals) in space; γ [dimensionless] the time index; and λ [T^{-1}] the truncation parameter in time.

The time index, γ which is between 0 and 1 in this study, is a parameter unique to the t-fADE which controls the power law distribution of solute particle waiting times. During waiting periods, solute particles remain motionless, representing the effect of immobilization within dead

zones (Zhang et al. 2009). As γ is small and approaches 0 (representing a higher probability for long waiting times), a larger portion of the solutes become trapped in the immobile phase, resulting in the apparent late time tail of the solute BTC.

The truncation parameter λ is concerned with the late time tail of tracer breakthrough curves. It adjusts the portion of power-law distributed waiting times and is responsible for the transition from power law to exponential waiting times, which naturally occurs as the concentration declines (Cartea A. et al. 2007, Rosinski 2007). When λ approaches infinity, the t-fADE model (1) reduces to the classical ADE model, which is applicable for either a homogeneous system or asymptotic transport where all relevant scales of heterogeneities have been experienced by solutes. In this way, the time index and truncation parameter of the t-fADE model are able to account for both subdiffusion and Gaussian asymptotic diffusion, and the many intermediate states between them. Therefore, it is our expectation that the t-fADE model may release dispersion from scale dependency; however, this fundamental assumption has never been tested.

3. APPLICATION

BTCs were obtained from two data sets including small scale, 1 meter and 12 meter intermediate scale, laboratory sand columns. For comparison, the t-fADE and ADE were both applied to match the BTCs for the generation of velocity, dispersion, and dispersivity values. In addition, the t-fADE parameters β , γ , and λ were also fit to the measured BTCs, to capture late-time tailing behavior not captured by the local, standard ADE model.

3.1 Small Scale Experimental Data

The small scale data set was obtained from experiments conducted at the environmental science laboratory in the Hefei University of Technology. Two one-meter glass columns, of 4 cm diameter, were carefully packed, one with spherical glass beads 1.5 mm in diameter, the other with more heterogeneous angular quartz grains, 1-2 mm (**Figure 1**). BTCs were created by instantaneously injecting a tracer of 5 mL Brilliant Blue FCF (BBF) of 0.1 g/L concentration. Water flumes were connected to either end of the column, one for recharge and one for discharge of the water. The flumes were connected to piezometer tubes at each end in order to measure different flow rates by the inlet and outlet heads. The experiment was repeated several times with various flow rates, including 0.6, 1.0, and 1.4 mL/s by adjusting the head difference of the piezometers. Concentration measurements were taken from 0.5 m as detected by an ultraviolet visible light spectrophotometer. Then the cylinder was drained, washed with tap water and the experiment repeated with measurements being taken at the full meter mark. In total 12 experiments were done, resulting in 12 BTCs.

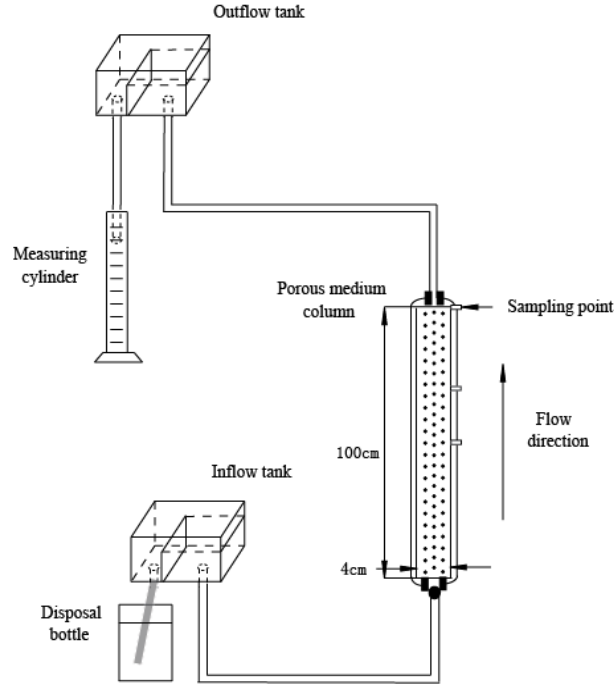


Figure 1. Set-up of the 1-meter columns.

The standard ADE model

$$\frac{\partial c}{\partial t} = -v \frac{\partial c}{\partial x} + D \frac{\partial^2 c}{\partial x^2}$$

was fit to the resulting BTCs using the solution expressed by equation 2 for an instantaneous source boundary condition at the inlet. The corresponding analytical solution is (see Charbeneau (2000), page 355, eq. (7.5.12)):

$$C(x, t) = \frac{M_0}{2\theta A \sqrt{\pi D t}} \exp\left[-\frac{(x-vt)^2}{4Dt}\right] \quad (2)$$

where M_0 [M] is the initial tracer mass, θ [dimensionless] is porosity, and A [L^2] is the cross-sectional area. For the standard ADE model without linear sorption/desorption, there is no distinction between mobile and immobile zones, and therefore there is only one porosity, with velocity (v) and the dispersion coefficient (D) being the two unknowns to be fit.

The t-fADE model (1), with the same boundary and initial conditions, was fit to the

BTCs after (1) was approximated by an implicit Eulerian finite difference solver modifying previous numerical schemes (Meerschaert and Tadjeran 2004; Zhang et al. 2015) (see Appendix). Five unknowns were solved, including velocity (v), dispersion (D), the time index (γ), the time truncation parameter (λ), and the capacity coefficient β , using guidelines from Zhang et al. (2015), detailed in the preceding methodology section. Velocity and dispersion are local variables, adjusted for each BTC. However, β and γ are plume scale variables, which were held constant over the length of the column but allowed to vary with flow rate. At this small scale, λ was insignificant and allowed to vary. Slope of the late-time BTC can be used to fit the value of index γ , while the overall expansion of late-time BTC defines β . Additional details of parameter fitting given BTCs can be found in Zhang et al. (2015). Values obtained from each model during the fitting process were tabled and compared using a conventional root mean square error (RMSE) analysis.

3.2 Intermediate Scale Literature Data

Intermediate scale BTC data was obtained from Huang et al.'s (1995) laboratory experiments which used two 12-m horizontal sand columns, of $10 \times 10 \text{ cm}^2$ cross sectional area, with different degrees of heterogeneity. Several hydrological models, including the s-fADE (Huang et al., 2008), have been tested with this data set, which however did not fit well the observed data (because the s-fADE assumes super-diffusive jumps without the capability to capture the ubiquitous retention). The homogeneous column was carefully packed with medium size sand grains while the heterogeneous column was made from a mix of cobbles, sand and interspersed clay lenses, having a coarse to fine grained trend, accompanied by increasing clay content and sediment layering (**Figure 2**). A NaCl tracer was continuously fed through the

columns. Measurements were taken every half meter in the homogenous column and every meter in the heterogeneous column, using electrical conductivity probes inserted laterally.

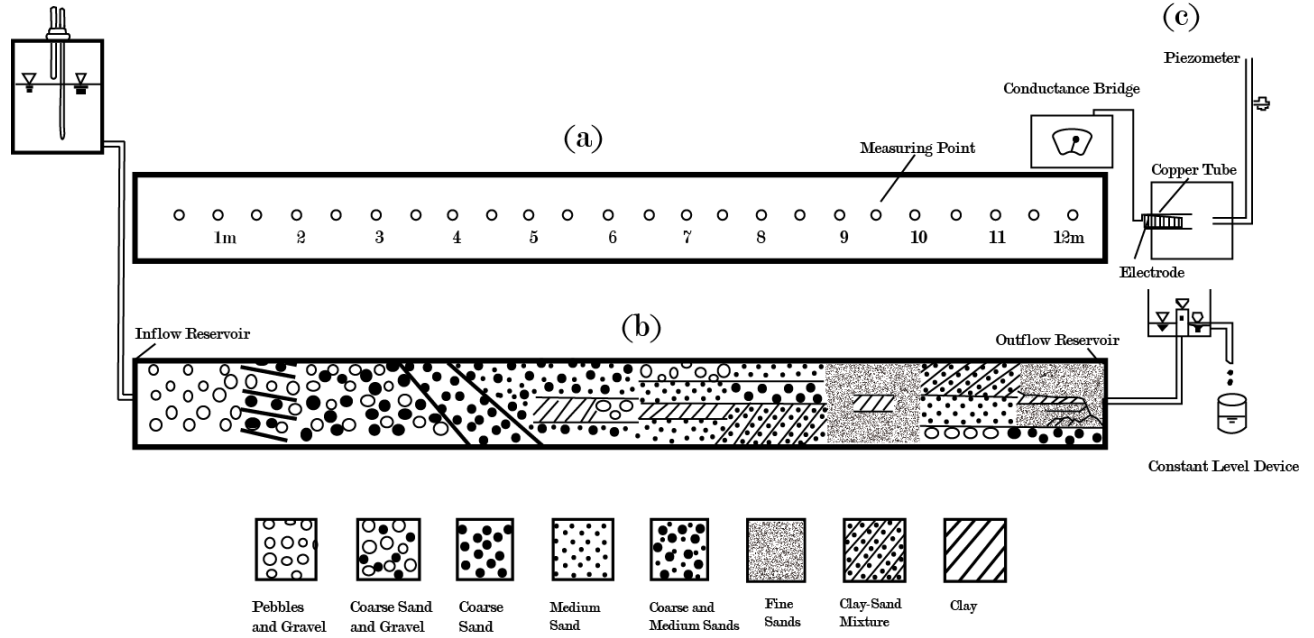


Figure 2. Intermediate Scale, heterogeneous column set-up. Figure adapted from Huang et al. (1995).

Here we modeled the BTCs with the ADE, using the continuous source boundary condition, the analytical solution being (see Charbeneau (2000), page 369, eq. (8.2.9)):

$$C(x, t) = 0.5 \operatorname{erfc}\left(\frac{x-vt}{\sqrt{4Dt}}\right) \quad , \quad (3)$$

where $\operatorname{erfc}()$ denotes the complementary error function. Velocity (v), and dispersion (D) were, again solved for, this time using Huang et al. (1995) as a guideline. Again, the Eulerian solver developed above (with an updated inlet boundary condition) was used to solve the t-fADE model. This time β , γ , and λ were all held constant across the length of each column, and only v and D were allowed to change locally. RMSE values were made by comparing the ADE and t-fADE to the sample concentration, to obtain quantitative evaluation of model fitting.

3.3 Issues comparing the t-fADE and ADE

Below is a discussion on the issues encountered when comparing the ADE to the t-fADE and how they have been addressed. First being the choice to keep the conventional ADE, without the addition of immobile water in the solutions. Following that is an explanation of the representative element volume (REV) and how it has been applied in this context; and finally, the relationship between the dispersion coefficient of the t-fADE and ADE, in this study, is detailed.

Although the purpose of comparing these two models is to determine the amount of influence retention has on the dispersion coefficient, it would not be appropriate to modify the ADE in order to account for immobilization. This is because the usage of the ADE model in this thesis is to identify whether column transport exhibits scale-dependent dispersion, not to prove that the single-rate mass transfer (SRMT) or MRMT model can fit the data. The t-fADE is a MRMT model with an upper-truncated, power-law rate coefficient, as demonstrated in the previous work (Zhang et al. 2015).

An explanation of the REV scale, for the ADE model (introduced by Bear (1972)), can be found in Charbeneau (2000) (page 9, equation (1.3.3)). The volume constituting the REV for assigning a value of the medium property should not be too small (so that the average value is not well defined) or too large (then soils with different textures may be mixed). However, a wide range of REV/grid size (from centimeters to kilometers) has been used in real-world models applying ADE-based approaches, while an appropriate REV size for the valid application of the ADE has not been systematically checked. For sandy soils, an averaging volume with a radius on the order of 10 to 20 grain diameters may lead to a well-defined average; while the REV can be as large as a basketball for heterogeneous porous media. In this thesis, I tested the

REV sizes increasing from 0.5 m to 12 m, to see whether the dispersion coefficient remained stable in the scales typically assumed to be valid for a REV. The REV size in the t-fADE should be more flexible than that in the ADE model, because the t-fADE was built upon the concept of a continuous time random walk which is valid at all relevant scales; see Metzler and Klafter (2000) and Meerschaert et al. (2008) for a theoretical background of the mathematical concept of CTRW and its link to fADE. For comparison purposes, the dispersion coefficient in the t-fADE is defined at the same REV scale as the ADE.

There is no established quantitative relationship between the dispersion coefficient (or dispersivity) in the ADE and the t-fADE (which is also one of the motivations for this work – wanting to compare them using laboratory BTCs), although the concept of dispersion remains the same in both models. Particularly, the dispersion coefficient in the ADE (denoted as D_A here) is a mathematical factor to scale the local displacement deviating from the mean advective drift due to mechanical dispersion and/or molecular diffusion. Hence the dispersion coefficient is a fitting parameter that can change with controlling factors including hydraulic conditions and pollutant chemical properties. In the t-fADE, the dispersion coefficient (denoted as D_t) captures the same mechanism as that in the ADE, with the only difference that the motion of pollutant particles described by the t-fADE can only occur in the mobile time (note that particles remain motionless in the immobile state). It is also noteworthy that, in this thesis, I adopt the same definition of “dispersivity” for the t-fADE model (i.e., $D_t = \alpha V$), for the purpose of direct comparison with the dispersivity in the ADE model.

4. RESULTS

4.1 Small Scale

Confirming previous research on the t-fADE, the model replicated BTC late time tailing, while the ADE assumed symmetrical Fickian diffusion (Meerschaert et al. 2008); see **Figure 3** and **Figure 4** for the glass-bead and quartz-grain column fittings, respectively. Likewise, full results of the model parameter fittings, including distance and flow rate, are listed in **Tables 1** and **2**. Results for both columns were similar despite differing grain and pore geometries. However, the model comparison results were not.

The ADE values for both dispersion and velocity increased with flow rate, resulting in relatively stable dispersivity. Note, however, that the standard ADE model cannot capture any late-time tailing behavior, observed in the tracer BTCs (**Fig. 3** and **4**), and therefore the best-fit ADE solution underestimates the real dispersion of solutes. Comparatively, the t-fADE model captures the overall trend of the BTCs, especially late-time tailing. The velocity and the dispersion coefficient in the t-fADE capture the motion of solute particles in relatively mobile zones. Again velocity increased with flow rate but a constant dispersion coefficient (0.0036 m²/hr) was achieved in both columns. Dispersivity held constant with travel distance but had an inverse relationship with flow rate, implying less variation from the mean flow at higher flow rates. The same inverse relationship was found for the capacity coefficient β , indicating that fewer solute particles were retained (or there were less immobile domains) as flow rate increased. The quartz column (with non-uniform size and irregularly shaped fill material) fit a

slightly greater β , suggesting comparatively greater immobilization than the (relatively uniform) glass-bead column. Likewise, the quartz column also fit a lower time index, γ , due to greater pore space heterogeneity and/or a larger specific surface area, allowing for more chemical sorption. The time parameter, λ , remained minimal at this scale due to the overall speed of transport.

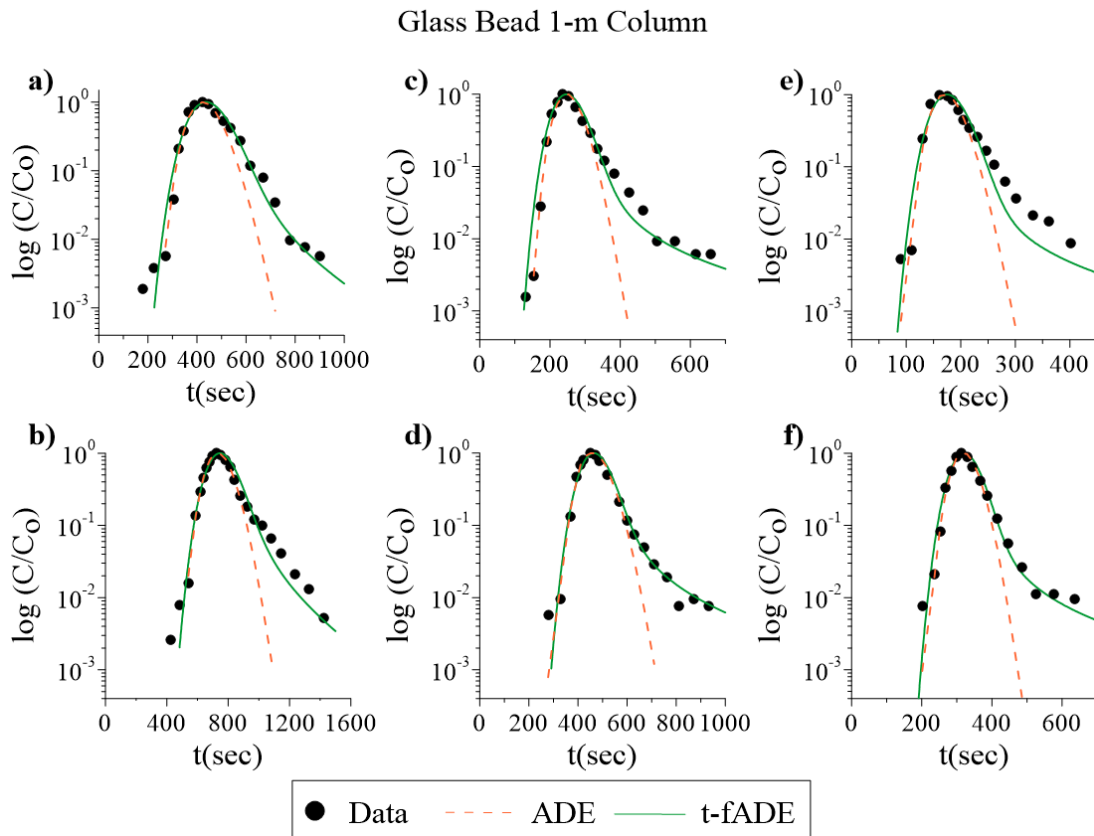


Figure 3. Fittings for the 1-m glass bead column. The half meter BTCs are above the full meter measurements for flow rates 0.6, 1.0, and 1.4 mL/s from left to right, respectively. The t-fADE captures the late time tailing behavior while the ADE solution, represented by dashed lines, assumes symmetry.

Table 1. Velocity, dispersion, and dispersivity values from the 1-m glass beads column. The best-fit t-fADE model parameters for each flow rate are also listed.

Runs		ADE				t-fADE						
flow rate (ml/s)	length (m)	v (m/hr)	D (m ² /hr)	α (m)	RM SE	v (m/hr)	D (m ² /hr)	α (m)	β (hr ^{γ-1})	γ	λ (hr ⁻¹)	RM SE
0.6	0.5	4.21	0.0216	0.005	2.4	4.28	0.0036	0.001	0.01	0.6	0.003	0.49
0.6	1.0	4.90	0.0288	0.006	5.3	5.00	0.0036	0.001	0.01	0.6	0.002	0.34
1.0	0.5	7.20	0.0360	0.005	7.7	7.63	0.0036	0.0005	0.009	0.6	0.0001	0.66
1.0	1.0	7.74	0.0540	0.007	3.9	7.99	0.0036	0.0005	0.009	0.6	0.0005	0.26
1.4	0.5	10.44	0.0576	0.006	7.7	10.62	0.0036	0.0003	0.007	0.6	0.0001	0.51
1.4	1.0	11.23	0.0648	0.006	7.3	11.52	0.0036	0.0003	0.007	0.6	0.0001	0.51

Table 2. Velocity, dispersion, and dispersivity values from the 1-m quartz grain column. The best-fit t-fADE model parameters for each flow rate are also listed.

Runs		ADE				t-fADE						
flow rate (ml/s)	length (m)	v (m/hr)	D (m ² /hr)	α (m)	RM SE	v (m/hr)	D (m ² /hr)	α (m)	β (hr ^{γ-1})	γ	λ (hr ⁻¹)	RM SE
0.6	0.5	4.86	0.0216	0.004	9.4	5.18	0.0036	0.0007	0.015	0.55	0.001	0.64
0.6	1.0	4.97	0.0216	0.004	5.2	5.26	0.0036	0.0007	0.015	0.55	0.005	0.46
1.0	0.5	7.92	0.0432	0.005	8.9	8.28	0.0036	0.0004	0.014	0.55	0.002	0.34
1.0	1.0	8.57	0.0324	0.004	9.8	9.00	0.0036	0.0004	0.014	0.55	0.004	0.79
1.4	0.5	10.44	0.0612	0.006	12.1	11.16	0.0036	0.0003	0.012	0.55	0.004	0.63
1.4	1.0	11.16	0.0504	0.005	13.1	11.52	0.0036	0.0003	0.012	0.55	0.008	0.53

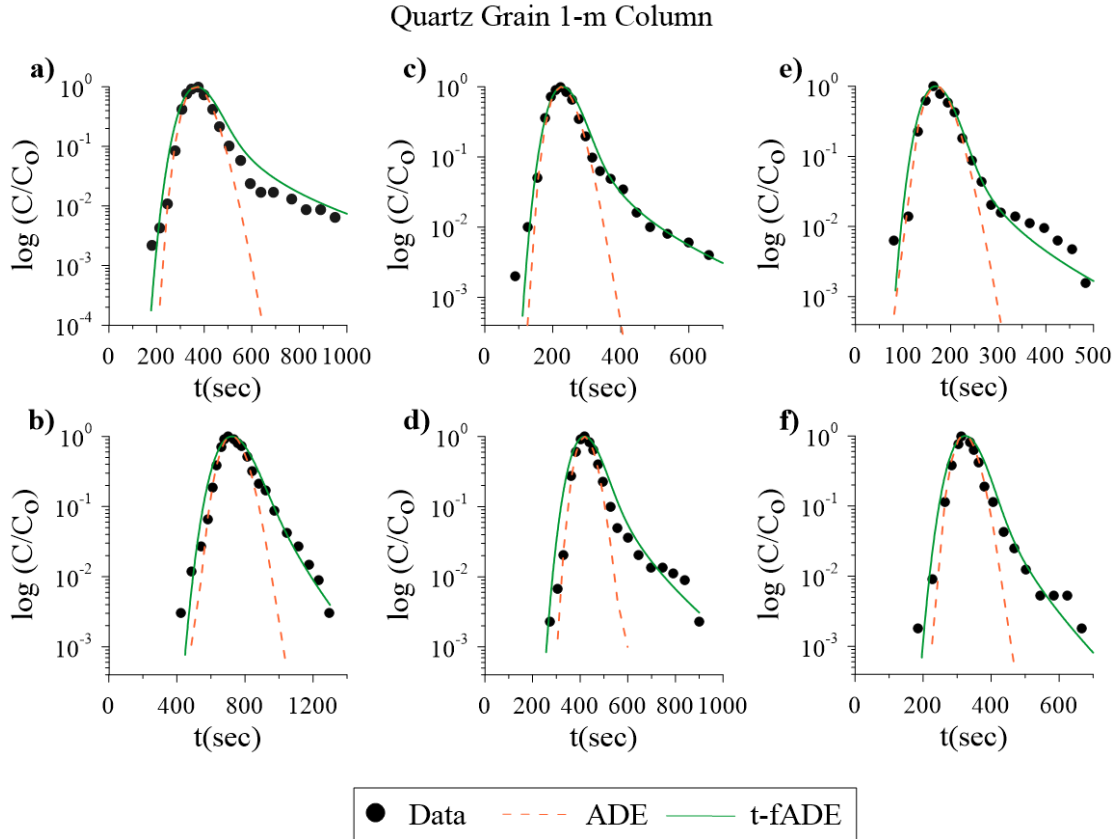


Figure 4. Fittings for the 1-m quartz grain column. The half meter BTCs are above the full meter measurements for flow rates 0.6, 1.0, and 1.4 mL/s from left to right, respectively. The t-fADE captures the late time tailing behavior while the ADE solutions shown by dashed lines assume symmetry.

4.2 Intermediate Scale

As there is less apparent tailing in BTCs measured from continuous source tracers, there is negligible differences between the ADE and t-fADE fittings in the homogeneous column (**Figure 5**). Full parameter fitting results including, velocity, dispersion, and dispersivity (which affect the mobile component for solute particles), for the homogenous column, are listed in **Table 3**, again noting little difference between the two models. The t-fADE's velocity is slightly higher due to the removal of immobile particles from the calculation for average velocity (**Figure 7a**). Unexpectedly, by meter 10.5 the t-fADE values for dispersion and dispersivity

begin to outpace the ADE, a consequence of β 's sensitivity to flow rate (as discovered in the small scale results) and the column's decreasing flow rate reported by Huang et al. (1995).

Table 3. Velocity, dispersion, and dispersivity values from the 12-m homogeneous sand column.

Runs	ADE				t-fADE			
length (m)	v (m/hr)	D (m²/hr)	α (m)	RMSE	v (m/hr)	D (m²/hr)	α (m)	RMSE
0.5	0.34	0.0010	0.0029	0.33	0.359	0.0007	0.0019	0.16
1.0	0.36	0.0012	0.0034	0.19	0.375	0.0010	0.0027	0.14
1.5	0.36	0.0009	0.0026	0.27	0.380	0.0008	0.0021	0.24
2.0	0.37	0.0014	0.0038	0.12	0.385	0.0013	0.0034	0.092
2.5	0.36	0.0017	0.0047	0.10	0.378	0.0017	0.0045	0.10
3.0	0.36	0.0025	0.0069	0.14	0.382	0.0023	0.0060	0.13
3.5	0.36	0.0020	0.0056	0.20	0.378	0.0020	0.0053	0.11
4.0	0.36	0.0042	0.012	0.13	0.379	0.0033	0.0087	0.13
4.5	0.36	0.0031	0.0090	0.45	0.375	0.0030	0.0080	0.50
5.0	0.35	0.0048	0.014	0.16	0.375	0.0042	0.011	0.18
5.5	0.36	0.0054	0.015	0.10	0.378	0.0050	0.013	0.076
6.0	0.36	0.0050	0.014	0.18	0.380	0.0042	0.011	0.24
6.5	0.34	0.010	0.028	0.25	0.360	0.008	0.022	0.30
7.0	0.34	0.010	0.029	0.11	0.360	0.008	0.022	0.066
7.5	0.34	0.011	0.032	0.061	0.361	0.010	0.028	0.047
8.0	0.34	0.013	0.038	0.061	0.358	0.013	0.036	0.059
8.5	0.33	0.014	0.042	0.11	0.350	0.013	0.037	0.16
9.0	0.34	0.011	0.032	0.14	0.360	0.011	0.031	0.17
9.5	0.34	0.011	0.032	0.31	0.357	0.011	0.031	0.33
10.0	0.34	0.013	0.039	0.48	0.354	0.013	0.037	0.46
10.5	0.34	0.015	0.045	0.18	0.352	0.018	0.051	0.14
11.0	0.33	0.013	0.039	0.043	0.348	0.015	0.043	0.034
11.5	0.33	0.015	0.045	0.070	0.352	0.016	0.045	0.053
12.0	0.34	0.018	0.054	0.049	0.356	0.018	0.051	0.048

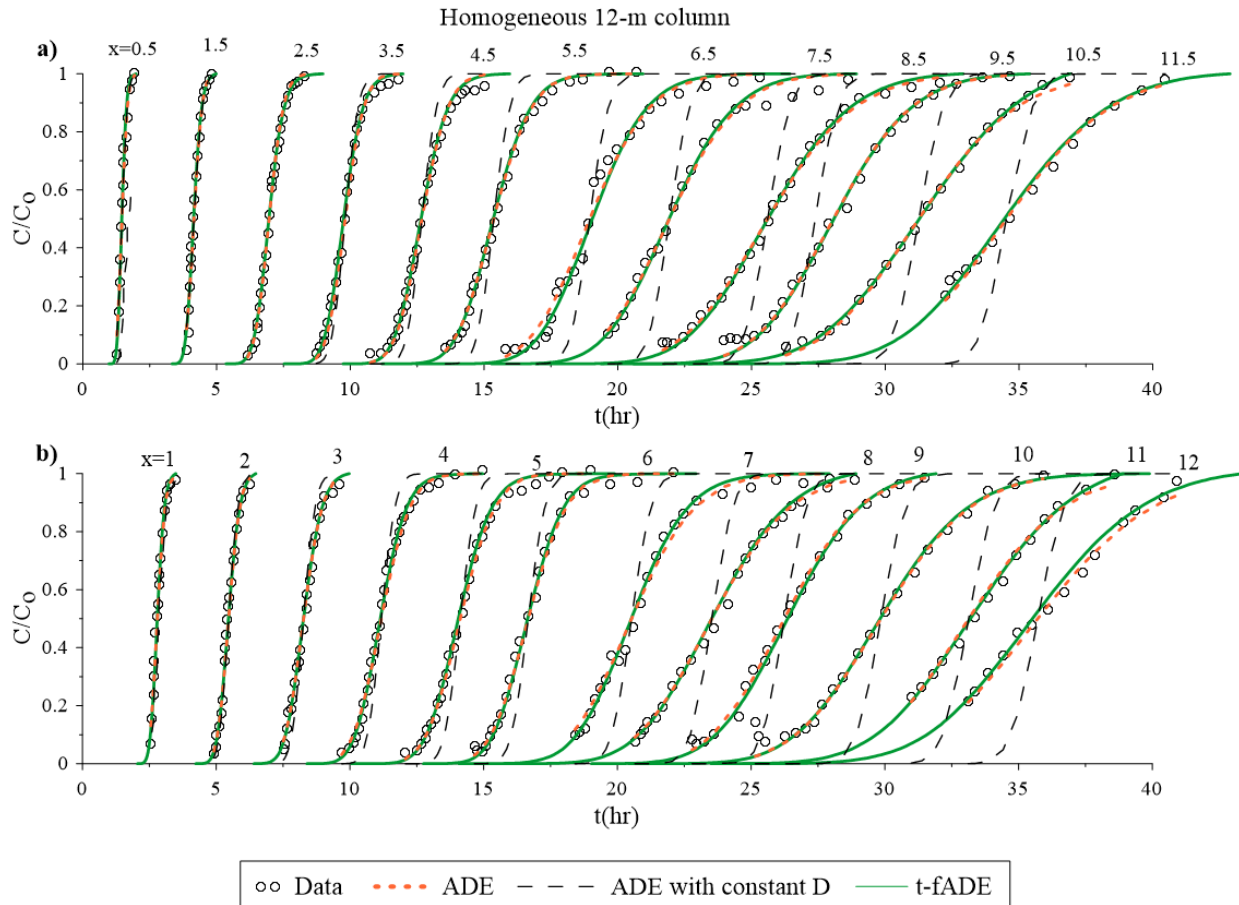


Figure 5. Fit of the t-fADE (solid lines) on the 12-m homogeneous column at half meter intervals. The t-fADE model fit is similar if not identical to the ADE because it is advection dominated with limited retention, which the ADE can't model. The best-fit solution of ADE is shown by dotted lines, and the predicted BTC using the ADE with constant dispersivity (estimated by the first BTC sampled at $x = 0.5\text{m}$) is showed by the long-dashed lines.

Conversely, there is greater tailing in the heterogeneous column (**Figure 6**) which challenged the ADE (and its applicability) but was well-fit by the t-fADE. The first two meters of the column were noticeably advective. Meters 3-6 are characterized by BTCs with distinct advective phases, where a majority of the concentration passed through quickly, followed by a much slower transport rate dominated by dispersion. It is this section of the column, where tailing is most apparent, that the ADE is unable to keep pace with the abrupt transition. Meters 7-12, making up the second half of the column, exhibited a more a gradual concentration

increase, implying greater dispersion in space. The ADE is successful in this portion of the column, where the transport mode remains consistent. On the other hand, the t-fADE was able to fit all sections of the column equally well. The resulting fitting values listed in **Table 4**, for the heterogeneous column, were strongly affected by the medium's heterogeneity, being much more volatile than the homogenous column. The t-fADE manages to reach a constant dispersion and dispersivity for the 3-6m region except when interrupted by clay lenses (at 3.5m) and a major clogging event at 8m (Huang et al. 1995). However, after this event, transport through the finer grained second half of the column, saw dispersion increase to values comparable with the ADE and remain so throughout the remainder of the column. In most cases, the RMSE values of the t-fADE are apparently smaller than those for the ADE, showing a better fit for the former.

It is noteworthy that, by visualization, there is a good fit of the ADE model at the travel distances $x = 2, 4, \text{ and } 8 \text{ m}$. At these locations, however, the measured BTC typically misses the late-time data, which is one of the core sections distinguishing Fickian and non-Fickian diffusion (or the ADE and t-fADE models). It is not clear if the ADE solution would fit the data well if the measurement was complete. Further studies are hence needed to obtain complete and accurate laboratory data to check the feasibility and scale-dependency of dispersion coefficient in the ADE and the t-fADE.

Table 5 lists the β , γ , and λ parameter fittings for the t-fADE model. The homogeneous column being more homogeneous registered a greater time index γ (representing a smaller probability for long trapping times) than the heterogeneous column. It also fit a larger λ , indicating a faster transition from power-law function to exponential in the late-time BTC. The capacity coefficient β was lower for the heterogeneous column, representing fewer solutes being retained in immobile zones.

Table 4. Velocity, dispersion, and dispersivity values from the 12-m heterogeneous sand column.

Runs	ADE				t-fADE			
length (m)	ν (m/hr)	D (m ² /hr)	α (m)	RMSE	ν (m/hr)	D (m ² /hr)	α (m)	RMSE
1	0.67	0.020	0.030	6.3	1.5	0.010	0.007	0.0134
2	0.68	0.11	0.16	0.54	0.83	0.070	0.084	0.18
3	0.64	0.08	0.13	0.23	0.79	0.010	0.013	0.28
3.5	0.63	0.15	0.24	0.13	0.79	0.070	0.089	0.087
4	0.65	0.10	0.15	0.23	0.79	0.010	0.013	0.16
5	0.70	0.18	0.26	0.13	0.87	0.010	0.011	0.13
6	0.69	0.20	0.29	0.10	0.87	0.010	0.011	0.055
7	0.56	0.60	1.1	0.066	0.73	0.60	0.82	0.074
8	0.55	1.2	2.2	0.45	0.85	1.00	1.2	0.088
9	0.59	0.50	0.85	0.10	0.80	0.30	0.38	0.088
10	0.53	0.45	0.85	0.082	0.72	0.30	0.42	0.057
11	0.53	0.70	1.3	0.088	0.75	0.50	0.67	0.071
12	0.52	0.50	0.96	0.081	0.72	0.50	0.69	0.070

Table 5. Values for β , γ and λ (in the t-fADE model) held constant for each 12-m column.

Parameter	Homogenous	Heterogeneous
β (hr ^{γ-1})	0.06	0.2
γ	0.9	0.55
λ (hr ⁻¹)	0.5	0.001

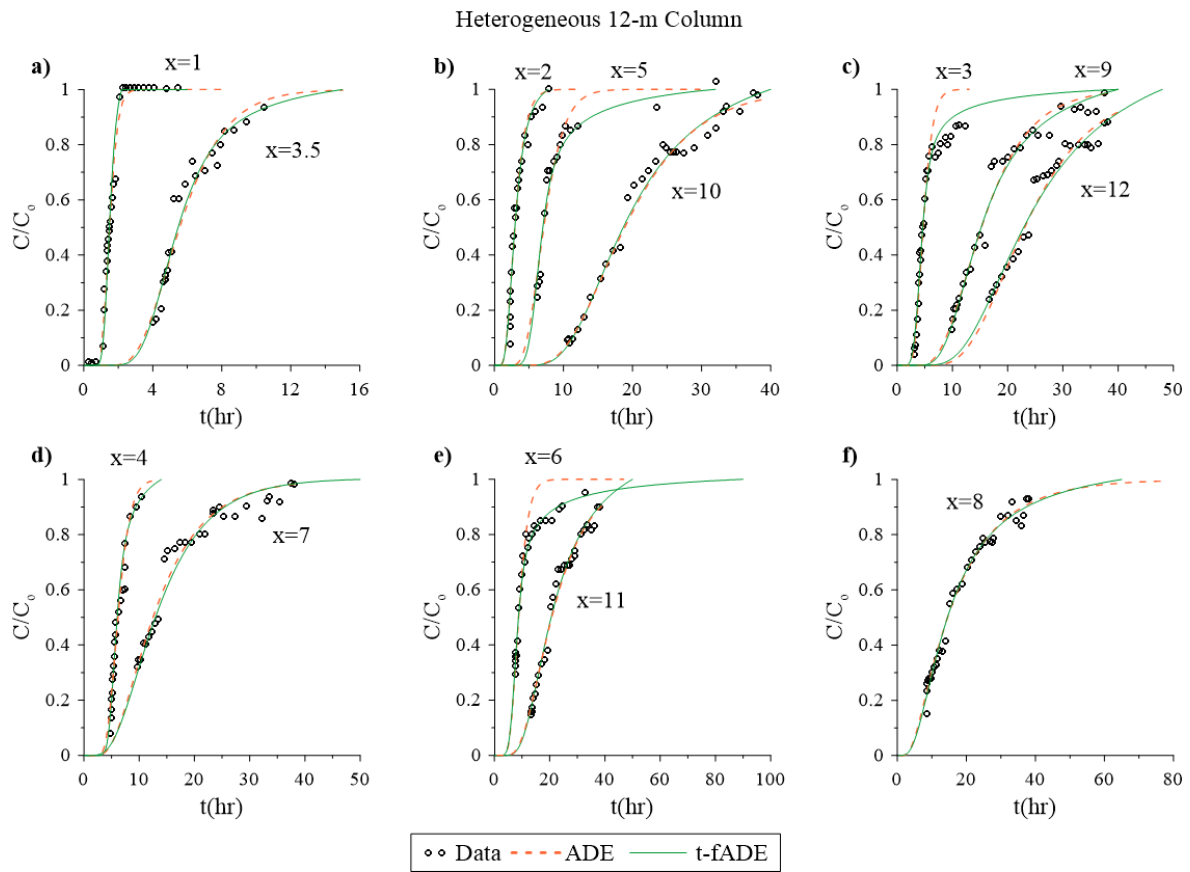


Figure 6. Fit of the t-fADE on the 12-m heterogeneous column at meter intervals. The t-fADE is able to model the transition from advection to dispersion (heavy tail) most noticeably at meters 3, 5, and 6, in contrast to the ADE.

5. DISCUSSION

Following is an evaluation of the applicability of the t-fADE model in capturing scale-dependent, non-Fickian dispersion for conservative tracer transport in saturated porous media, based on laboratory experimental data and the model analysis results shown above. Two directly correlated topics, including extension to other time nonlocal models and potential solutions for the identified scale problem, and discrepancy between laboratory experiments, are also discussed below. Finally, the possible future development of numerical models will be addressed, in reference to the results found in this thesis work.

5.1 The t-fADE Model Cannot Capture Scale-Dependent Dispersion

The t-fADE model (1) with a constant dispersion coefficient cannot capture the scale-dependent transport of conservative tracers in the 12-m heterogeneous sand column (**Figure 8b**), although this model, as with other time-nonlocal transport models including the well-known MRMT model (Haggerty et al. 2000) and the CTRW framework (Berkowitz et al. 2006), can efficiently describe the late-time tailing of non-Fickian transport. The dispersion coefficient in the t-fADE (1) must increase nonlinearly with travel distance for both the heterogeneous and (macroscopically) homogeneous sand columns. Pre-asymptotic non-Fickian transport can be persistent in repacked sand columns, as shown by **Figures 8 and 9**.

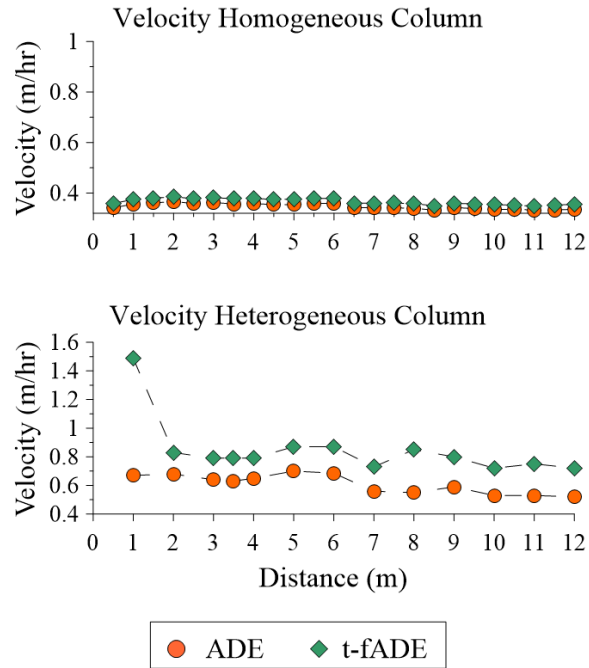


Figure 7. Best-fit velocity at the 12-m intermediate scale. Greater velocity at the start of the heterogeneous column is due to macropores near the injection site.

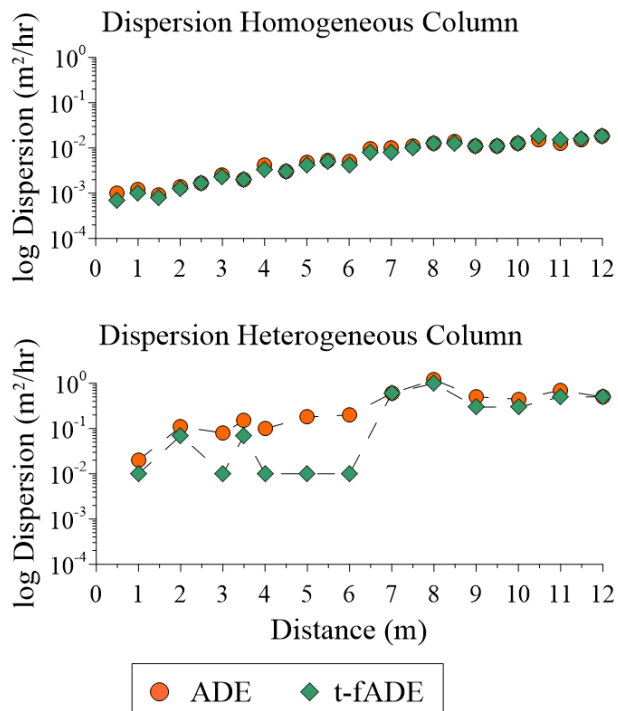


Figure 8. Best-fit log dispersion at the 12-m intermediate scale. The same scale is used for both columns.

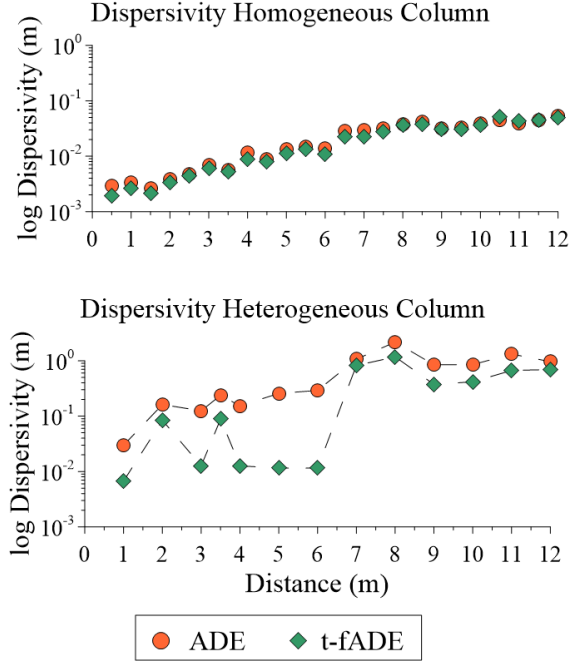


Figure 9. Best-fit log dispersivity at the 12-m intermediate scale. Increases are seen in both columns but the heterogeneous column experiences more volatility.

The scale-dependency of dispersivity in the t-fADE may be related to the physical properties of the model. Following the argument in Zhang et al. (2009), the t-fADE model (1) can be decomposed into mobile and immobile processes described by:

$$\frac{\partial p(x, m)}{\partial m} = -v \frac{\partial p(x, m)}{\partial x} + D \frac{\partial^2 p(x, m)}{\partial x^2} \quad (4a)$$

$$\frac{\partial h(m, t)}{\partial m} = -\frac{\partial h(m, t)}{\partial t} - \beta e^{-\lambda t} \frac{\partial^\gamma [e^{\lambda t} h(m, t)]}{\partial t^\gamma} \quad (4b)$$

where m and t denote the motion time and the total time, respectively. Eq. (4a) describes a motion process with a number density p , and Eq. (4b) governs a hitting time process with density h . In other words, the spatial jump of solute particles described by (4a) is defined by two transport parameters – velocity v (defining the advective displacement in mobile time m) and the dispersion coefficient D (defining Fickian jumps during m), while the retention process of solutes

in immobile zones described in (4b) is controlled by three time-domain parameters (β , γ , and λ). The solute concentration C follows the conditioning argument: $C(x, t) = \int_0^\infty p(x, m)h(m, t)dm$. On one hand, the three time-domain parameters capture solute retention and the corresponding stretching of the solute plume in space, resulting in a non-linear evolution of the plume's mean and variance (and therefore non-Fickian transport). On the other hand, the two transport parameters control the mean drift (due to the mean velocity) and local fluctuation due to the deviation of local velocity from the mean, where the scaling factor of this spatial fluctuation (which is the dispersion coefficient D) is assumed to be constant in the t-fADE (1). However, for real-world transport processes, a solute particle moving through the medium can experience various local-scale medium heterogeneity (even with a macroscopically homogeneous sand column) where the velocity distribution can expand with increasing spatial size (Baeumer et al. 2001). Therefore, the dispersion coefficient D may no longer remain stable, but is more likely to increase with travel distance, propagating non-Fickian transport that cannot be accounted for by the mechanism of solute retention.

To further check if the observed transport was scale dependent, the experiment was re-run with the standard ADE using a constant dispersivity to fit the BTC measured at all sampling locations along the 12m-long homogeneous sand column. Results (represented by the long-dashed lines in **Figure 5**) show that the dispersion coefficient which fit the BTC at small travel distances underestimates the BTC at a larger distance x , and this discrepancy increases with an increasing distance. Hence, transport in the homogeneous column is scale dependent. In addition, the best-fit result using both the ADE and t-fADE also shows that the dispersivity is not a constant (for local or intermedia scale transport) or a linear function of the travel distance, but rather a variable increasing nonlinearly with the travel distance even for the relatively

“homogeneous” sand column (**Figure 9**). Therefore, there may not be a real medium that is strictly “homogeneous”, even for well-prepared sand columns in the laboratory. All natural media should be heterogeneous, with the only difference being in degree and scale, resulting in the spatial evolution of flow velocity and triggering scale-dependent dispersion.

5.2 Comparison to Other Models and Possible Solutions for Scale-Dependent Dispersion

Other time-nonlocal transport models may suffer the same scale-dependent issue with the dispersion coefficient. For example, the MRMT model also separates solute dynamics into mobile and immobile components, similar to equations (4); for details, see Haggerty et al. (2000). Therefore, the dispersion coefficient in the MRMT model may increase with travel distance when solute particles gradually encounter more regions of the host medium and sample a broader velocity distribution. The t-fADE (1), considered in this thesis, is a specific MRMT model using a truncated, power-law distribution for rate coefficients, which is functionally equivalent to the CTRW framework with an exponentially truncated, power-law memory function. The scale issue identified in this study for the t-fADE could be common for similar time-nonlocal physical models separating mobile jumps and waiting periods.

Efficiently releasing time-nonlocal transport models from scale-dependency, therefore, becomes a major challenge for practical applications. There may be three possible solutions for promising fractional-derivative models. First, one can add a spatial fractional-derivative term to the t-fADE (1), resulting in a spatiotemporal fADE model (Zhang et al. 2015). The spatiotemporal fADE can capture both retention and the early-arrivals of solutes; therefore it may characterize scale-dependent dispersion due to mobile particles gradually sampling a wider distribution of velocities. However, this potential improvement may not be ideal since the resultant model necessitates the use of additional parameters. A second possible method is to

extend the time index in the t-fADE (1) from a range of 0~1 to 1~2, so that the t-fADE model can capture both slow and fast displacement of solute particles (Meerschaert et al. 2010). The final solution is to apply the subordination approach, proposed by Baeumer et al. (2001) and Zhang et al. (2014), to capture the fast movement of solute particles (driven by mechanical dispersion) along streamlines. These three potential solutions are key areas for future study.

5.3 Discrepancy between Small- and Intermediate-Scale Laboratory Experiments, and Potential Impact of Water Flow Rate on Scale-Dependent Dispersion

The small-scale sand column experiments showed different transport dynamics from the historical, 12-m long sand columns built by Huang et al. (1995). The 1-m, small-scale laboratory experiments were conducted to compensate for deficiencies in the intermediate-scale transport experiment by 1) providing details in the late-time BTC tailing (due to use of an instantaneous point source) which was not shown clearly in the intermediate-scale transport experiment (where the continuous source overshadowed the nuance of the solute particles late-arrivals in the BTC), and 2) evaluating the impact of water flux on non-Fickian dynamics. However, transport results from the small-scale sand column results differ from the intermediate-scale column. Particularly, the 1m-long sand column experiments did not reveal apparent scale-dependency for the dispersion coefficient D in the t-fADE, although the 1-m long homogeneous sand column identified much stronger retention in solute transport than the 12m-long homogeneous sand column in Huang et al. (1995).

A possible explanation for the above discrepancy may stem from the specific hydrologic conditions adopted in our experiments. For example, the relatively large velocity in the 1m-column (which is one-order-of-magnitude larger than the 12m-column) might flush most solutes out of the short column quickly, limiting the chance/time for mobile solute particles to

experience the full spectrum of local velocities and generate apparent scale-dependent dispersion. The scale impact on transport was therefore minimized. This assumption may also explain why the glass-beads and quartz-sand columns share similar dispersivity values in the ADE model, while they actually contain different pore geometries and internal structures. Secondly, in the 1m-long column experiments, a small number of solute particles might be trapped near the instantaneous point source, due to the solute injection mode which may force some solute particles moving into relatively low-velocity zones (i.e., immobile zones) at the initial source area. This behavior is analogous to the “sequestration” effect (LaBolle and Fogg 2001), which can result in a tracer BTC with delayed tailing. This sequestration phenomenon also expands the solute plume in space, because the plume front is flushed downstream quickly at the same time, extending the whole plume in space. The stretched plume can be easily confused with scale-dependent dispersion if the standard ADE model is used, where an increasing dispersion coefficient is required. The t-fADE model can, however, correctly capture the retention process and the late-time tailing in the BTC due to retention, and therefore does not require any large or scale-dependent dispersion coefficient to capture the overall stretched plume. Additional experiments with lower water flow rates and different injection modes are needed to further check the above two hydrologic conditions in the future, and most importantly, explore the potential impact of water flux on the scale-dependency of dispersion.

5.4 Dispersivity as a Linear Regression

Dispersivity measurements from these experiments have been added to the Gelhar et al. (1992) plot for log dispersivity with log distance (**Figure 10**). Since the work of Arya et. al. (1988), Neuman (1990), and more recently Schulze-Makuch (2005), a universal scaling law relationship has been sought between α and transport scale by means of linear regression. Such a

scaling law would allow a correlation to exist between concentration measurements from various field or laboratory data. Gelhar et al. (1992)'s work combining data from 59 sites provided a superficial trend. However, this trend is skewed by the repetition of some sites. A more recent analysis of the plot by Zech et al. (2015) removed repeat and low reliability data from the plot and added additional recent data. Their plot loses the overall trend but sees α remain in the range of 0.45-10.5 m (or $\log 10^{-1}$ to 10^1 m) from the scale of 0.5 to 100m. This confirms the general trend of dispersivity but does not support a universal linear regression.

Rather, as supported by the four column experiments (**Figure 10**), while each system exhibited an increasing trend of α with scale, the initial α value did not depend on the scale of the system. In this thesis, this unique trend holds true for both the t-fADE and the ADE. An exception is the very low α values of the t-fADE in the 1-m columns for the reasons discussed in section 5.3. Although a universal linear regression is potentially possible for all systems, α trends from the t-fADE, in this thesis do not offer a solution.

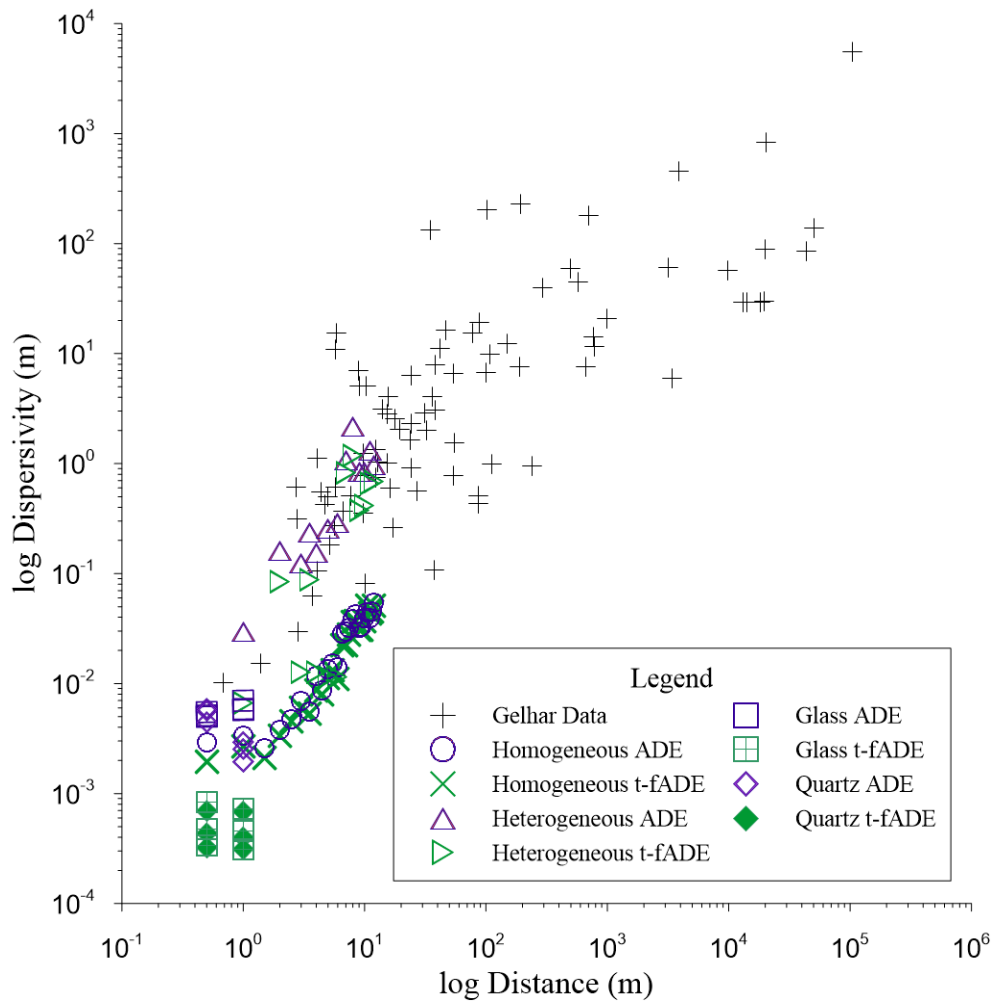


Figure 10. A log-log plot of dispersivity with distance from all four column experiments. This is combined with data from Gelhar et. al. (1992), which includes data from 59 field sites.

5.5 Do we need a paradigm shift in numerical modeling of non-Fickian transport?

Stochastic methods have been developed by hydrologists to describe solute transport in heterogeneous media for ~40 years, but these models usually exhibit poor predictability and lack hydrogeologic information; see extensive discussion by Cirpka and Valocchi (2016), Fiori et al. (2016), Fogg and Zhang (2016), Rajaram (2016), and Sanchez-Vila and Fernandez-Garcia (2016). This study found that the time nonlocal transport model (with constant parameters), as one of the popular stochastic models, might be further challenged by scale-dependent dispersion. Considering the “structure of scientific revolutions” proposed by Kuhn (1962) and quick development in hydrologic sciences (Clifford, 2002), is a “paradigm shift” required where new transport theories should be developed to replace the advection-dispersion equation and stochastic models (including the t-fADE) with limited applications?

One example of the paradigm shift is the advection-diffusion model with matrix diffusion (Gillham et al. 1984; Hadley and Newell 2014), which is applicable for nonreactive tracer transport in layered aquifers where transverse molecular diffusion can significantly affect the mean travel velocity and dominate late-time mass decline. The well-known stochastic macro-dispersion model may not be applicable for this case because of the relatively short travel distance (Molz 2015) and the persistent pre-asymptotic transport. Similar channelized models with slow advection and apparent Taylor dispersion has also been proposed by other researchers (Becker and Shapiro 2003) and checked against Monte Carlo simulations (LaBolle and Fogg 2001; Zhang et al. 2007). These studies confirm that mechanical dispersion in the governing equation is negligible if the numerical model can capture the layered distribution of hydraulic conductivity or channeling velocity. For regional-scale transport processes with limited subsurface information or intermediate-scale repacked sand columns without a layering

structure, mechanical dispersion might still be needed to explain the local deviation from mean velocity (Baeumer et al., 2015).

This thesis provides useful information for both a possible “paradigm shift” and updating previous stochastic models in capturing the nuance of anomalous transport. On one hand, the t-fADE model, has been found similar to the other time-nonlocal transport models (note that the t-fADE is actually a general time-nonlocal model as suggested by Cvetkovic (2011)), in that it cannot capture scale-dependent dispersion caused by local velocity variation. In other words, if non-Fickian transport is caused by both the time memory effect (i.e., mass exchange between the high and low permeability layers, as identified by the advection-diffusion model) and the spatial evolution of local flow velocity, then the latter mechanism needs to be accounted for in previous time nonlocal transport models such as the t-fADE, MRMT, and the hydrologic-version of the CTRW model. On the other hand, if the advection-diffusion model is used to account for layered media with strong spatial variations of water flux in interconnected channels, differential advection might be characterized with caution since it can add additional fluctuation to the leading front of plumes. Most importantly, there is a need to incorporate major aquifer information, especially aquifer connectivity and architecture, into the numerical model, as suggested by various researchers (Fogg and Zhang 2016; Rajaram 2016; Sanchez-Vila and Fernandez-Garcia 2016). The above information can be incorporated into the multi-dimensional hydrofacies model using Markov chain based geostatistical tools (Carle and Fogg 1997), where the horizontal grid size (representing the REV for the classical ADE model) was empirically defined as at least one order of magnitude smaller than the horizontal correlation scale of the hydrofacies while the vertical size of the grid should be smaller than the smallest mean thickness of all hydrofacies. This approach captures transport with skewed BTCs in regional-scale multi-

dimensional heterogeneous aquifers (Weissmann et al. 2002), but is not applicable for the one-dimensional (homogeneous) sand column utilized by this study.

The dilemma of the “paradigm shift” is entangled by the hypothesis that the applicability of transport models in capturing complex transport dynamics may depend on the resolution of the flow field, or the REV scale for the classical ADE model. For example, if the pore-scale velocity can be mapped, the classical ADE can capture complex, scale-dependent dispersion with a constant diffusion coefficient. In addition, one can adjust the mean velocity in the advection-diffusion model using the tortuosity factor proposed for the stream tube model (Clennell 1997; Ghanbarian et al. 2013; Berg 2014), and therefore a constant diffusion coefficient (combined with variable velocities) may capture scale-dependent dispersion induced by differential advection. For one-dimensional transport processes, the ideal way to quantify scale-dependent dispersion due to mechanical dispersion is to keep a constant velocity and upscale dispersion as suggested by the three solutions in section 5.3, where several upscaling, stochastic techniques can be tested to derive a final model with a constant dispersion coefficient to capture scale-dependent dispersion. Hence the limitation of the t-fADE and related time-nonlocal models identified by this work might be fixed in the future, without the need for paradigm shift.

6. CONCLUSION

The t-fADE, a time nonlocal stochastic model, was tested in this study for its capability in capturing scale-dependent, non-Fickian transport in saturated porous media. BTCs were obtained from laboratory sand columns of varying heterogeneity, flow rate, and scale (1-meter vs 12-meters in length). It was found that the t-fADE model with a constant dispersion coefficient cannot capture the scale-dependent transport of conservative tracers in the 12-m heterogeneous sand column, although it can efficiently describe the late-time tailing of non-Fickian transport. Indeed, the dispersion coefficient increased nonlinearly with the travel distance, likely due to local velocity variations, rather than retention. This held true regardless of the macroscopic degree of heterogeneity. An exception being at the small scale (i.e., the 1-m sand columns built in our laboratory), where a relatively large water flux may have overshadowed the variation of local velocities, or experimental conditions may have caused significant sequestration near the injection site, which could exhibit a substantial impact on the overall growth of plume, outweighing local conditions.

The issue of the dispersion coefficient's scale-dependency may extend beyond the t-fADE to other time nonlocal models which separate statistical parameters describing waiting time retention and spatial jump advection. Although retention is modelled at the plume scale, local velocities defining spatial jumps (forming advection dominated transport zones) can vary independent of solute retention dynamics. Improvements on time nonlocal models are necessary to incorporate the spatial evolution of local velocities without adding cumbersome parameters, which remains a fundamental challenge.

REFERENCES

- Arya, A., T.A. Hewett, R.G. Larson, L.W. Lake. "Dispersion and Reservoir Heterogeneity." *SPE Reservoir Engineering*, vol. 3 no. 1, 1988, pp. 139-148.
- Axelsson, O., and I. Gustafsson. "A modified upwind scheme for convective transport equations and the use of a conjugate gradient method for the solution of non-symmetric systems of equations." *IMA Journal of Applied Mathematics*, vol. 23, no. 3, 1979, pp. 321-337.
- Baeumer, B., M.M. Meerschaert, D.A. Benson, and S.W. Wheatcraft. "Subordinated advection-dispersion equation for contaminant transport." *Water Resources Research*, vol. 37, no. 6, 2001, pp. 1543-1550.
- Baeumer, B., Y. Zhang, and R. Schumer. "Incorporating super-diffusion due to sub-grid heterogeneity to capture non-Fickian transport." *Groundwater*, vol. 53, no. 5, 2015, pp. 699-708.
- Bear, J. *Dynamics of Fluids in Porous Media*. Elsevier, New York, USA. 1972
- Becker, M.W., and A.M. Shapiro. "Interpreting tracer breakthrough tailing from different forced-gradient tracer experiment configurations in fractures bedrock." *Water Resources Research*, vol. 39, no. 1, 2003, Art. No. 1025, doi:10.1029/2001WR001190.
- Benson, D.A., S.W. Wheatcraft, and M.M. Meerschaert. "The fractional-order governing equation of Levy motion." *Water Resources Research*, vol. 36, no. 6, 2000, pp. 1413-1423.
- Berg, C.F. "Permeability description by characteristic length, tortuosity, constriction and porosity." *Transport in Porous Media*, vol. 103, no.3, 2014, pp. 381-400.
- Berkowitz, B., A. Cortis, M. Dentz and H. Scher. "Modeling non fickian transport in geological formations as a continuous time random walk." *The American Geophysical Union: Reviews of Geophysics*, vol. 44, no. 2, 2006, pp. 1-49.
- Beven, K. "Towards a new paradigm in hydrology." *International Association of Hydrological Sciences: Proceeding from the Rome Symposium*, no. 164, 1987, pp. 393-403.
- Beven K. "On modelling as collective intelligence." *Hydrological Processes*, vol. 15, 2001, pp. 2205-2207.

- Cardenas, M. B. "Direct simulation of pore level fickian dispersion scale for transport through dense cubic packed spheres with vortices." *The American Geophysical Union: Geochemistry Geophysics Geosystems*, vol.10, no. 12, 2009, pp.1-8.
- Carle, S.F. and G.E. Fogg. "Modeling spatial variability with one and multidimensional continuous-lag Markov chains." *Mathematical Geology*, vol. 29, no.7, 1997, pp. 891-918.
- Cartea A. and D. del-Castillo-Negrete. "Fluid limit of the continuous-time random walk with general Levy jump distribution functions." *Physical Review E*, vol. 76, 2007, pp. 1-8. 041105
- Charbeneau, R.J. *Groundwater Hydraulics and Pollutant Transport*. Upper Saddle River, NJ: Prentice Hall, 2000.
- Chaudhary, K., M. B. Cardenas, W. Deng and P. C. Bennett. "Pore geometry effects on intrapore viscous to inertial flows and on effective hydraulic parameters." *Water Resources Research*, vol. 49, 2013, pp. 1149-1162.
- Cirpka, O.A., and A.J. Valocchi. "Debates-Stochastic subsurface hydrology from theory to practice: Does stochastic subsurface hydrology help solving practical problems of contaminant hydrogeology?" *Water Resources Research* vol. 52, no. 12, 2016 pp. 9218-9227. doi:10.1002/2016WR019087.
- Clennell, M.B. "Tortuosity: a guide through the maze." *Geological Society, London, Special Publications*, vol. 122, no. 1, 1997, pp. 299-344.
- Clifford, N.J. "Hydrology: the changing paradigm." *Progress in Physical Geography* vol. 26, no. 2, 2002, pp. 290-301.
- Coats, K. H., and B. D. Smith. "Dead-end pore volume and dispersion in porous media." *Society of Petroleum Engineers Journal*, vol. 4, 1964, pp. 73-84.
- Cushman, J. H. "Stochastic filtering of multiphase transport phenomena." *Transport in Porous Media*, vol. 2, 1987, pp. 425-453.
- Cushman, J.H. "A primer on upscaling tools for porous media." *Advances in Water Resources* vol. 25, 2002, pp. 1043-1067.
- Cvetkovic, V. "The tempered one-sided stable density: A universal model for hydrological transport?" *Environ Res Lett* vol. 6, 2011, 034008, doi:10.1088/1748-9326/6/3/034008.
- Dagan G. "Stochastic modeling of groundwater flow by unconditional and conditional probabilities: 2. The solute transport." *Water Resources Research*, vol. 18, 1982, pp. 835-848.
- Dagan, G. *Flow and transport in porous formations*. Heidelberg Berlin: Springer-Verlag, 1989.

- Fiori, A., V. Cvetkovic, G. Dagan, S. Attinger, A. Bellin, P. Dietrich, A. Zech, and G. Teutsch. "Debates-Stochastic subsurface hydrology from theory to practice: The relevance of stochastic subsurface hydrology to practical problems of contaminant transport and remediation. What is characterization and stochastic theory good for?" *Water Resources Research*, vol. 52, no. 12, 2016, pp. 9228-9234. doi:10.1002/2015WR017525.
- Fogg, G. E., and Y. Zhang. "Debates-Stochastic subsurface hydrology from theory to practice: A geologic perspective." *Water Resources Research*, vol. 52, no. 12, 2016, pp. 9235-9245. doi:0.1002/2016WR019699.
- Garabedian, S. P., L.W.Gelhar, and M.A.Celia. "Large-Scale Dispersive Transport in Aquifers: Field Experiment and Reactive Transport Theory. Ralph M. Parsons Laboratory." *Hydrology and Water Resource Systems*. Report Number 315, pp. 1988.
- Gelhar, L. W. and C.L. Axness "Three Dimensional Stochastic Analysis of Macrodispersion in Aquifers." *Water Resources Research*, vol. 19, 1983, pp. 161-180.
- Gelhar, L.W, C. Welty, and K.R. Rehfeldt. "A Critical Review of Data on Field-Scale Dispersion in Aquifers." *Water Resources Research*, vol. 28, no.7, 1992, pp.1955-1974.
- Gelhar, L.W. *Stochastic Subsurface Hydrology*. Prentice-Hall College Division, 1993.
- Ghanbarian, B., A.G. Hunt, R.P. Ewing and M. Sahimi. "Tortuosity in porous media: a critical review." *Soil Science Society of America Journal*, vol.77, no.5, 2013, pp. 1461-1477.
- Gillham, R.W., E.A. Sudicky, J.A. Cherry, and E.O. Frind. "An Advection-Diffusion Concept for Solute Transport in Heterogeneous Unconsolidated Geological Deposits." *Water Resources Research*, vol. 20, no. 3, 1984, pp. 369-378.
- Hadley, P.W., and C. Newell. "The New Potential for Understanding Groundwater Contaminant Transport." *Groundwater*, vol. 52, no. 2, 2014, pp. 174-186.
- Haggerty, R., and S.M. Gorelick. "Multiple-rate mass transfer for modeling diffusion and surface reactions in media with pore-scale heterogeneity." *Water Resources Research*, vol. 31, no. 10, 1995, pp. 2383-2400.
- Haggerty, R., S.A. McKenna and L.C. Meigs. "On the late-time behavior of tracer test breakthrough curves." *Water Resources Research*, vol. 36, no. 12, 2000, pp. 3467-3479.
- Haggerty, R., C.F. Harvey, C.F.V. Schwerin and L.C. Meigs. "What controls the apparent timescale of solute mass transfer in aquifers and soils? A comparison of experimental results." *Water Resources Research*, vol. 40, no 1., 2004, W01510,doi:10.1029/2002WR001716.
- Hess, K. M., S. H. Wolf and M. A. Celia. "Large scale natural gradient test in sand and gravel, Cape Cod Massachusetts 3. Hydraulic conductivity variability and calculated macrodispersivities." *Water Resources Research*, vol. 28, no. 8, 1992, pp. 2011-2027.

- Huang, K., N. Toride, and M.T. Van Genuchten. "Experimental investigation of solute transport in large, homogenous and heterogeneous, saturated soil columns." *Transport in Porous Media*, vol. 18, 1995, pp. 283-302.
- Huang, Q., G.Huang, and H. Zhan. "A finite element solution for the fractional advection–dispersion equation." *Advances in Water Resources*, vol. 31, 2008, pp. 1578-1589.
- Koch D. and J. Brady. "Dispersion in Fixed Beds." *Journal of Fluid Mechanics*, vol. 154, 1984, pp. 399-427.
- Kuhn, T.S. "The Structure of Scientific Revolutions." *International Encyclopedia of United Science*, vol. 2, no. 2, 1962, pp. 1-210.
- LaBolle, E.M., and G.E. Fogg. "Role of Molecular Diffusion in Contaminant Migration and Recovery in an Alluvial Aquifer System." *Transport in Porous Media*, vol. 42, 2001, pp. 155-179.
- Lowe, C.P., and D. Fenkel. "Do Hydrodynamic Dispersion Coefficients Exist?" *The American Physical Society*, vol. 77, no. 22, 1996, pp. 4552-4555.
- Meerschaert, M.M., and C. Tadjeran. "Finite difference approximations for fractional advection–dispersion flow equation." *Journal of Computational and Applied Mathematics*, vol. 172, 2004, pp. 65–77.
- Meerschaert, M.M., Y. Zhang and B. Baeumer. "Tempered Anomalous Diffusion in Heterogeneous Systems." *Geophysical Research Letters*, vol. 35, no. 9, 2008, L17403, DOI:10.1029/2008GL034899.
- Meerschaert, M.M., Y. Zhang and B. Baeumer. "Particle tracking for fractional diffusion with two time scales." *Computers and Mathematics with Applications*, vol. 59, no. 3, 2010, 1078-1086, doi:10.1016/j.camwa.2009.05.009.
- Metzler, R. and J. Klafter. "The Random Walk's Guide to Anomalous Diffusion: A Fractional Dynamics Approach." *Physics Reports*, vol. 339, 2000, pp. 1-77.
- Molz, F. "Advection, Dispersion, and Confusion." *Groundwater*, vol. 53, no. 3, 2015, pp. 348-353.
- Neuman, S.P. "Universal Scaling of Hydraulic Conductivities and Dispersivities in geologic Media." *Water Resources Research*, vol. 26, no. 8, 1990, pp. 1749-1758.
- Neuman, S. P. and V. Di Federico. "Multifaceted Nature of Hydrogeologic Scaling and its Interpretation." *American Geophysical Union: Review of Geophysics*, vol. 41, no 3, 2003, pp. 4-1,4-31.
- Neuman, S.P., and D.M. Tartakovsky. "Perspective on theories of non-Fickian transport in heterogeneous media." *Advances in Water Resources*, vol. 32, 2009, pp. 670-680.

- Pachepsky, Y., D. Benson and W. Rawls. "Simulating scale-dependent solute transport in soils with the fractional advective–dispersive equation." *Soil Science Society of America Journal*, vol. 64, 2000, pp. 1234-1243.
- Pickens, J.F., and G.E. Grisak. "Modeling of scale-dependent dispersion in hydrogeologic systems." *Water Resources Research*, vol. 17, no. 6, 1981, pp. 1701-1711.
- Rajaram, H. "Debates-Stochastic subsurface hydrology from theory to practice: Introduction." *Water Resources Research*, vol. 52, no. 12, 2016, pp. 9215-9217, doi:10.1002/2016WR020066.
- Rosinski, J. "Tempering stable processes." *Stochastic Processes and their Applications*, vol. 117 no. 2, 2007, pp. 677-707.
- Sanchez-Vila X., and D. Fernandez-Garcia. "Debates – Stochastic subsurface hydrology fro, theory to practice: Why stochastic modeling has not yet permeated into practitioners?" *Water Resources Research*, vol. 52, no.12, 2016, 9246-9258. doi:10.1002/2016WR019302.
- Schulze-Makuch, D. "Longitudinal dispersivity data and implications for scaling behavior," *Ground Water*, vol. 43, no. 3, 2005, pp. 443–456, doi:10.1111/j.1745-6584.2005.0051.x.
- Schumer, R., D.A. Benson, M.M. Meerschaert, and B. Baeumer. "Fractal Mobile/immobile solute Transport." *Water Resources Research*, vol. 39, no. 10, 2003, pp. 1296-1338.
- Serrano, S. E. "Forecasting scale-dependent dispersion from spills in heterogeneous aquifers." *Journal of Hydrology*, vol. 169, 1995, pp. 151-169.
- Sun, H., W. Chen, C. Li and Y. Chen. 2012. "Finite difference schemes for variable-order time fractional diffusion equation." *International Journal of Bifurcation and Chaos*, vol. 22, no. 4, 2012, 1250085: 1-16.
- Van Genuchten, M. Th. and P.J. Wierenga. "Mass Transfer Studies in Sorbing Porous Media I. Analytical Solutions." *Soil Science Society of America Journal: Division S-1—Soil Physics*, vol. 40, no 4, 1979, pp. 473-480.
- Van Wesenbeeck, I.J., and R.G. Kachanoski. "Spatial scale dependence of in situ solute transport." *Soil Science Society of America*, vol. 55, no. 1, 1991, pp. 3-7.
- Wei, S., W. Chen and J. Zhang. "Time-fractional derivative model for chloride ions sub-diffusion in reinforced concrete." *European Journal of Environmental and Civil Engineering*, vol. 21, no. 3, 2015, pp. 319-331.
- Weissmann, G.S., Y. Zhang, E.M. LaBolle and G.E. Fogg. 2002. "Dispersion of groundwater age in an alluvial aquifer system." *Water Resources Research*, vol. 38, no. 10, 2002, pp. 1198, doi:10.1029/2001WR000907.

- Zech, A., S. Attinger, V. Cvetkovic, G. Dagan, P. Dietrich, A. Fiori, Y. Rubin, and G. Teutsch. “Is unique scaling of aquifer macrodispersivity supported by field data?” *Water Resources Research*, vol. 51, 2015, pp. 7662–7679, doi:10.1002/2015WR017220.
- Zhang, D. *Stochastic methods for flow in porous media: Coping with uncertainties*. San Diego, California: Academic Press. ISBN 012-7796215, 2002.
- Zhang, Y., D.A. Benson, and B. Baeumer. “Predicting the tails of breakthrough curves in regional-scale alluvial systems.” *Ground Water*, vol. 45, no. 5, 2007, pp. 473-484.
- Zhang, Y., D.A. Benson and D.M. Reeves. “Time and space nonlocalities underlying fractional-derivative models: Distinction and literature review of field applications.” *Advances in Water Resources*, vol. 32, 2009, pp. 561-581.
- Zhang, Y., R.L. Martin, D. Chen, B. Baeumer, H. Sun, and L. Chen. “A subordinated advection model for uniform bed load transport from local to regional scales.” *Journal of Geophysical Research - Earth Surface*, vol. 119, 2014, pp. 2711–2729, doi:10.1002/2014JF003145.
- Zhang, Y., M.M. Meerschaert, B. Baeumer and E.M. LaBolle. “Modeling mixed retention and early arrivals in multidimensional heterogeneous media using an explicit Lagrangian scheme.” *Water Resource Research*, vol. 51, pp. 6311–6337, DOI:10.1002/2015WR016902.
- Zheng, C., M. Bianchi and S.M. Gorelick. “Lessons learned from 25 years of research at the MADE site.” *Groundwater*, vol. 49, no. 5, 2011, pp. 649-662.
- Zhou, L. and H. M. Selim. “Scale-dependent dispersion in soils: An overview.” *Advances in Agronomy*, vol. 80, 2003, pp. 223-263.

APPENDIX

Finite Difference Solution for the T-fADE model

Consider the t-fADE model (1) with the following boundary condition

$$L_b u(\mathbf{x}, t) = g(\mathbf{x}, t) \quad (\text{A1})$$

and initial condition

$$u(\mathbf{x}, 0) = f(\mathbf{x}) \quad (\text{A2})$$

where L_b represents the boundary operator. The operator $\frac{\partial^\alpha}{\partial t^\alpha}$ in (1) is the Caputo definition of a fractional derivative, which is stated as (Wei et al. 2015)

$$D_t^\alpha f(t) = \frac{\partial^\alpha f(t)}{\partial t^\alpha} = \frac{1}{\Gamma(1-\alpha)} \int_0^t \frac{f'(\tau)}{(t-\tau)^\alpha} d\tau, \quad 0 < \alpha < 1 \quad (\text{A3})$$

The Crank-Nicholson finite-difference scheme is utilized in this study, inasmuch as it has been proven to achieve high accuracy and unconditional stability for solving fractional equations (Meerschaert and Tadjeran 2004; Sun et al. 2012). In addition, it is well known that numerical diffusion occurs when the convective term in the advection-dispersion equation is discretized with a first order accurate, finite-difference scheme (Axelsson and Gustafsson 1979). In order to alleviate the numerical diffusion issue, a second-order upwind scheme is employed.

Here the spatial domain is first discretized using $x_i = idx$, with $0 \leq i \leq N$, $Ndx = L$, and dx as the space step length. The time domain is then discretized as $t_j = jdt$, with $0 \leq j \leq M$, $Mdt = T$, and dt is the time step size. The symbol $C(x_i, t_j) = C_i^j$ denotes the concentration at grid points $x_i = idx$ and $t_j = jdt$.

The discretization of the Caputo definition can be stated as follow

$$\frac{\partial^\alpha C(x_i, t_{j+1})}{\partial t^\alpha} \approx \begin{cases} a_0 (C_i^{j+1} - C_i^j) + a_0 \sum_{k=1}^j b_k (C_i^{j-k+1} - C_i^{j-k}), & j \geq 1 \\ a_0 (C_i^1 - C_i^0), & j = 0 \end{cases} \quad (\text{A4})$$

where $a_0 = \frac{(dt)^{-\alpha}}{\Gamma(2-\alpha)}$, $b_k = [(k+1)^{1-\alpha} - k^\alpha]$, ($k = 1, 2, \dots, j$).

The second-order upwind scheme is defined as

$$C_x^- = \frac{\partial C_i^j}{\partial x} \approx \frac{3C_i^j - 4C_{i-1}^j + C_{i-2}^j}{2dx} \quad (\text{A5})$$

$$C_x^+ = \frac{\partial C_i^j}{\partial x} \approx \frac{-C_{i+2}^j + 4C_{i+1}^j - 3C_i^j}{2dx} \quad (\text{A6})$$

For convenience of implementation, equation (A5) is applied for formula derivation thereafter.

The diffusion term in the t-fADE model (1) is then discretized using the Crank-Nicholson scheme:

$$\frac{\partial^2 C_i^j}{\partial x^2} \approx \frac{1}{2} \left[\frac{C_{i+1}^{j+1} - 2C_i^{j+1} + C_{i-1}^{j+1}}{dx^2} + \frac{C_{i+1}^j - 2C_i^j + C_{i-1}^j}{dx^2} \right] \quad (\text{A7})$$

Substituting (A4), (A5) and (A7) into (1), the finite difference discretization form of the t-fADE model is obtained:

$$\begin{cases} P_1 C_{i-2}^{j+1} - P_2 C_{i-1}^{j+1} + P_3 C_i^{j+1} - P_4 C_{i+1}^{j+1} = -Q_1 C_{i-2}^j + Q_2 C_{i-1}^j + Q_3 C_i^j + Q_4 C_{i+1}^j - Q_5, & j \geq 1 \\ P_1 C_{i-2}^1 - P_2 C_{i-1}^1 + P_3 C_i^1 - P_4 C_{i+1}^1 = -Q_1 C_{i-2}^0 + Q_2 C_{i-1}^0 + Q_3 C_i^0 + Q_4 C_{i+1}^0, & j = 0 \end{cases} \quad (\text{A8})$$

where $P_1 = \frac{V}{4dx}$, $P_2 = \frac{D}{2dx^2} + \frac{V}{dx}$, $P_3 = \frac{1}{dt} + \beta a_0 + \frac{D}{dx^2} + \frac{3V}{4dx}$, $P_4 = \frac{D}{2dx^2}$, $Q_1 = \frac{V}{4dx}$, $Q_2 = \frac{D}{2dx^2} + \frac{V}{dx}$,

$$Q_3 = \frac{1}{dt} + \beta a_0 e^{-\lambda dt} - \frac{D}{dx^2} - \frac{3V}{4dx}, \quad Q_4 = \frac{D}{2dx^2}, \quad Q_5 = \beta a_0 e^{-\lambda t_{j+1}} \sum_k^j b_k \left(e^{\lambda t_{j-k+1}} C_i^{j-k+1} - e^{\lambda t_{j-k}} C_i^{j-k} \right). \quad \text{The}$$

second line in equation (A8) shows the solution for chemical concentrations at the first time step 1, given the boundary condition and the initial condition. The first line in equation (A8) provides a solution for (1) at all the remaining time steps.